Micro-channel heat exchanger optimization

Conference Paper · March 1991

DOI: 10.1109/STHERM.1991.152913 · Source: IEEE Xplore

2 authors, including:

George Harpole
Northrop Grumman
35 PUBLICATIONS **395** CITATIONS

MICRO-CHANNEL HEAT EXCHANGER OPTIMIZATION

George M. Harpole and James E. Eninger
TRW R1/1022, Redondo Beach, CA 90278

Abstract

Micro-channel heat exchangers consist of a small-scale finned surface etched in silicon and a manifold system to force liquid flow between the fins. A back-side manifolding concept is presented which allows cooling the entire footprint of the heat exchanger and stacking to cool large continuous areas. A numerical model of the multi-dimensional flow and heat transfer was developed and used to optimize the design parameters. The model shows that effective heat transfer coefficients on the order of 100 W/cm^{2}K can be achieved with pressure drops of only 1 or 2 bar.

Introduction

The present micro-channel concept is similar to the human cardiovascular system, with the micro-channels being analogous to the capillaries. The single coolant flow from the supply block (aorta) branches down in the distribution manifold (arteries), which feed many very small flows in the micro-channels (capillaries). At this level, there are hundreds of thousands of individual flows in the heat exchanger, each efficiently absorbing a fraction of a watt. The length scale is so small, that the temperature drop between the channel wall and the coolant is at most only a few degrees. After the heat is absorbed, the flows recombine in the distribution manifold (veins) and merge into a single outlet stream in the supply block (vena cava).

Micro-channel heat exchangers are fabricated by chemically etching narrow fins and channels in silicon. High-aspect-ratio, uniform channels and fins are easily etched in silicon (see Fig. 1 and [1]). With proper alignment, etching depths per lateral undercutting can be as large as 600:1. Fin and channel widths as narrow as 10 μm are practical. The flow is single phase (liquid) and is laminar. In laminar flow, the local heat transfer coefficients are inversely proportional to the coolant channel width. Moreover, the fins increase the effective surface area by an order-of-magnitude over that of the face sheet alone. A micro-manifold (also etched silicon) reduces pressure drops by several orders of magnitude. The manifold subdivides the flow so that: 1) the flow paths through the micro-channels are short (perhaps 0.3 mm) and 2) the local flow velocity is low.

The main features of this micro-channel concept are shown in Fig. 2. There are essentially three layers that are diffusion bonded together: the micro-channel face sheet, the coolant distribution manifold, and the coolant supply block. From the top down, each of these layers has larger and fewer channels than the ones above it, and the channels in each adjacent layer are rotated perpendicular with respect to the other. The manifold and coolant supply layers are shown in Fig. 3. Holes are etched to connect common (high or low) pressure regions between layers.

Surface emitting diode laser arrays that continuously dump 1 kW/cm^2 are the impetus for developing such a remarkable heat exchanger. Efficient laser operation requires surface temperatures below 25°C. Lateral surface temperature variations must be less than 1°C to maintain wavelength coherence between the lasing elements.

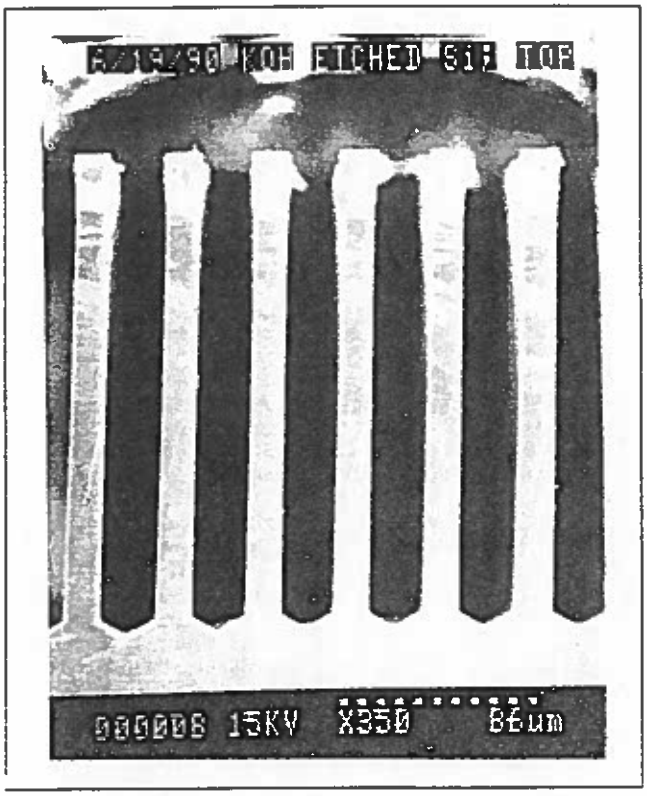

Fig.1 Micro-channels etched at TRW, 200 μm depth, 25 μm channel width, 15 μm fin thickness.

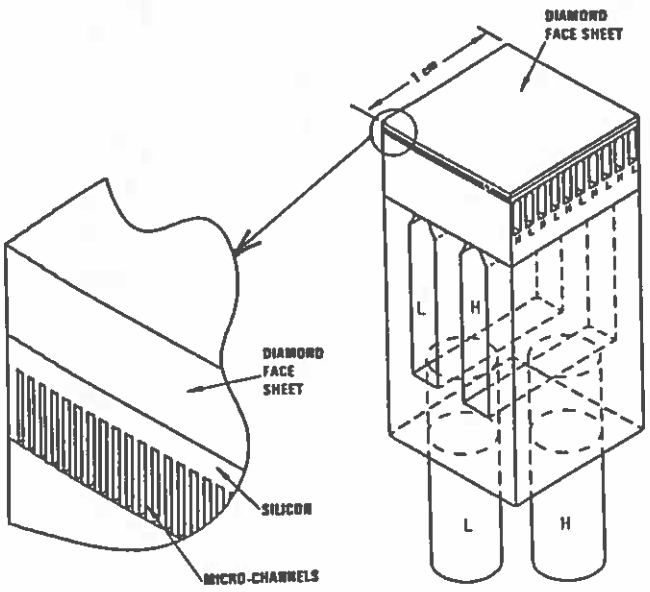

Fig.2 Micro-channel heat exchanger with a diamond face sheet.

CH2972-8/91/0000-0059 $1.00 ©1991 IEEE

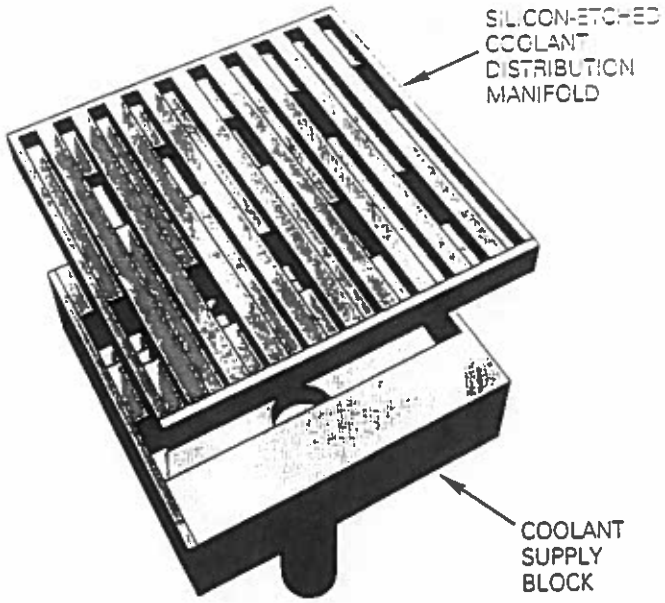

Fig.3 Silicon-etched coolant distribution manifold showing coolant supply passages.

Micro-channel heat exchangers were originally developed by Tuckerman [2], and have been further developed by Mundinger [3]. The present advances are: 1) a coolant distribution manifold that allows cooling the entire footprint of the heat exchanger, allowing stacking to cool large, continuous areas, 2) a diamond face sheet, to reduce lateral surface temperature variations, and 3) a two-dimensional flow and heat transfer model to optimize the many design parameters. This model and parameter optimization are the subject of the present paper. Up to this point, micro-channel heat exchangers have been designed on the basis of simple one-dimensional models, despite the two-dimensional nature of the flow.

Flow and heat transfer are solved in the top layers of the heat exchanger (diamond, silicon, and fins/coolant) shown in Fig. 4. A unit cell is taken between vertical symmetry lines through the center of a manifold inlet channel and the center of an exit channel. The flow field is needed to solve the convective heat transfer in the micro-channels. There are 7 geometrical parameters, a choice of coolant, and coolant flow rate to determine. The purpose of the present model is to provide a rational basis for choosing these parameters by optimization.

Flow Field

This low-Reynolds-number flow is laminar, inertia is negligible, and entrance length effects are negligible. Low-Reynolds-number flow between parallel plates is called "Hele-Shaw flow." It follows Darcy's law for flow in porous media with a permeability of $K=\delta_c^2/12$, where δ_c is the micro-channel width. This permeability was determined from the parabolic velocity profile across the width of the micro-channel (in z). The subject of this section is determining the dependence of the velocity vector on the other two dimensions (x and y).

With no inertia, conservation of momentum is expressed as $v = -K\nabla p/\mu$, where v is the velocity vector, p is pressure, and μ is viscosity. Conservation of mass is expressed as $\nabla \cdot v = 0$. Conservation of mass and momentum combine to give Laplace's equation, $\nabla^2 p = 0$. The boundary conditions are specified pressures in the inlet and exit manifolds at the bottom of the micro-channels and no penetration (zero normal velocity, thus, zero normal pressure gradient) at the solid boundaries (top and part of bottom) and at symmetry lines (vertical lines centered over the inlet and exit).

An infinite series expansion in terms of "cos" and "cosh" with arbitrary coefficients was found that satisfies Laplace's equation and the top, left, and right boundary conditions. The coefficients were determined by a least squares fit to the bottom boundary conditions. In dimensionless (normalized) form, these solutions depend only on two parameters: the aspect ratios H_F/L and W/L. Related series expansions then give the local velocity vector components, the total volume flow rate, and the stream function. Fig. 4 shows one flow field that was generated by this mathematical solution. The isobars (dashed lines) are lines of constant pressure (20 equal divisions between the inlet and exit pressure). Streamlines (solid lines, 10 equal divisions of the total volume flow) are paths traced by individual fluid particles.

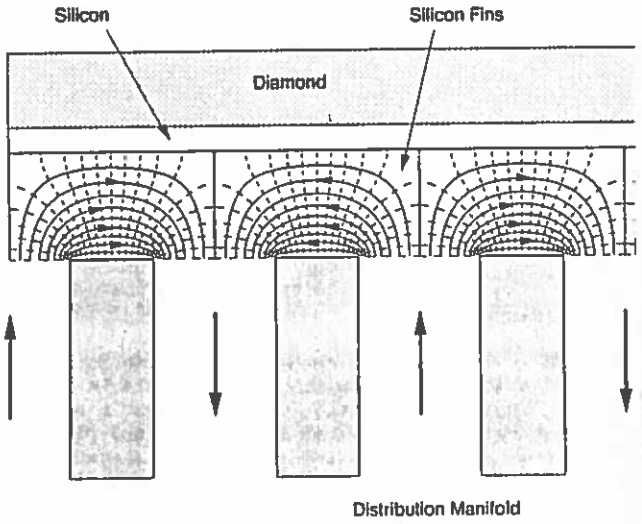

Fig.4 Top layers showing coolant flow in micro-channels and manifold.

Heat Transfer

The local energy balance in the coolant within the micro-channels includes heat carried by the fluid in the direction of the velocity vector (advection) and heat exchange from the fins in proportion to the local temperature difference between the fins and the coolant. Heat diffusion through the coolant in the x-y plane is negligible. The energy conservation equation for the coolant is

$$\rho c_p v \cdot \nabla T_c = (T_f - T_c) hS/V_c$$

where ρ is coolant density, c_p is coolant specific heat, T_c is coolant temperature (averaged across the channel), T_f is fin temperature, h is the heat transfer coefficient, S is the total fin surface area, and V_c is the total coolant volume within the micro-channels. The velocity vector v is known from the flow field solution. The heat transfer coefficient is given by $h = Nu\ k_c/\delta_c$, where Nu is the Nusselt number, k_c is the coolant thermal conductivity, and δ_c is the micro-channel width. For fully developed laminar flow with a constant wall heat flux, Nu=8.24, while with a constant wall temperature, Nu=7.54. The

Nusselt number used here is Nu=8.1, because the constant heat flux condition for a given streamline is more nearly correct over most of the fin area, while the constant temperature condition is approached near the exit. The results are not very sensitive to the exact choice of Nu.

The coolant energy equation was solved by a finite-difference marching method using second-order (3 point) upwind differencing in x and y. This non-iterative method starts with the given coolant temperature at the inlet and marches in the flow direction to the exit.

The energy balance in the solid layers (diamond, silicon, and fins) includes heat diffusion in x and y. In the diamond and silicon layers, the energy conservation equation is $\nabla^2 T = 0$. In the fins, the energy balance also includes local heat exchange with the coolant. Temperature is nearly uniform through the fin thickness (z), because they are so thin. In the fins, the energy conservation equation is

$$k_{Si}\nabla^2 T_f = (T_f - T_c)hS/V_f$$

where k_{Si} is thermal conductivity of the silicon fins and V_f is the total volume of the fins.

This multi-region heat transfer in the solid was solved by the alternating direction implicit (ADI) iterative finite-difference method with 3-point central differencing in x and y. The coolant heat transfer solution was run between each iteration of the solid solution, because the solutions are coupled to each other. Sample isotherm contour maps for the coolant (Fig. 5) and the solid layers (Fig. 6) are shown for a particular case.

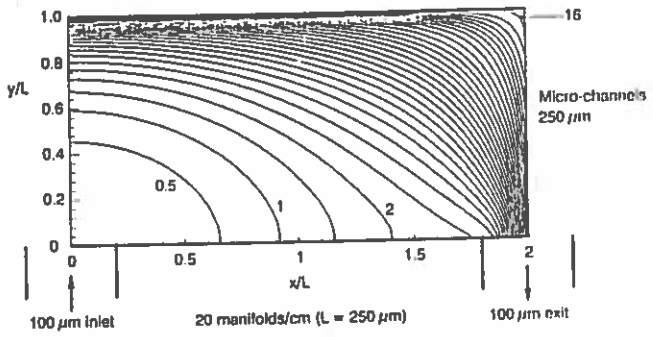

Fig.5 Isotherms in the coolant (0.5°C increments) 1 kW/cm2, 40 cc/s flow, 15 μm fins and channels.

Parameter Optimization

The complete flow/thermal model was run to the select the heat exchanger design parameters. Nine independent parameters must be selected: 1) coolant fluid, 2) coolant flow rate, 3) number of manifold channels per width, 4) fin height, 5) fin thickness, 6) micro-channel width, 7) inlet/exit width, 8) silicon layer thickness, and 9) diamond thickness (see Fig. 7). The goals are: 1) good lateral temperature uniformity, 2) low thermal resistance (high overall heat transfer coefficient), and 3) low coolant pump power (pressure drop and flow rate).

For comparison purposes, several of the parameters were kept fixed while others were varied. The coolant properties are for 80% water/20% methanol at 7°C (-15°C freezing point): 0.00217 kg/m.s viscosity, 0.48 W/m.K thermal conductivity, and 3.99×10^6 J/m^{3}K density times specific heat. After performing these calculations, it was realized that

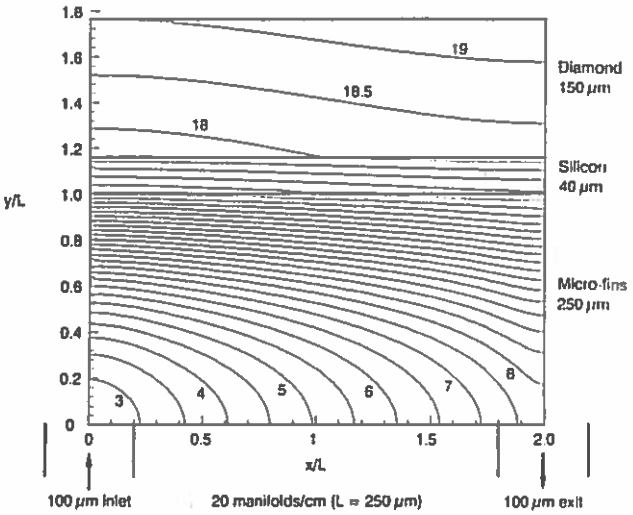

Fig.6 Isotherms in the solid (0.5°C increments), 1 kW/cm2, 40 cc/s, 15 μm fins and channels.

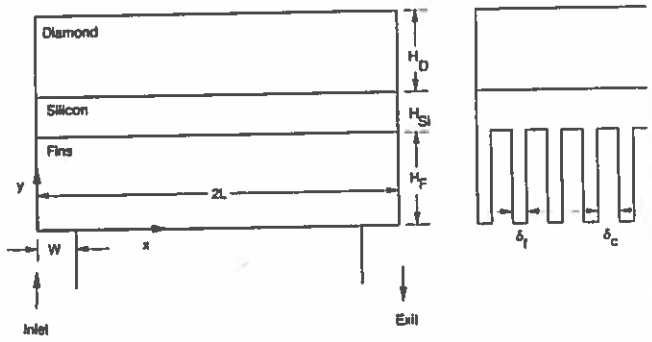

Fig.7 Length variable and coordinate definitions.

this much antifreeze was not necessary, and nearly pure water could be used. The primary difference with pure water as the coolant is half the viscosity, and thus, half the viscous pressure loss shown on the graphs (there are also small heat transfer advantages to pure water). The diamond layer thickness is 150 μm, the silicon layer thickness is 40 μm. The heat load is 1 kW/cm^2.

Consider a fixed pump power and allow the geometry and flow rate to vary within this constraint. Ideal pump power is pressure drop times volume flow rate. Thus, a 1 bar drop with 50 cc/s and a 2 bar drop with 25 cc/s both require 5 W ideal pump power (or 10 W for a 50% efficient pump). Fig. 8 shows the maximum lateral surface temperature variation for these two flow conditions as a function of the number of manifold channels for various fin heights, with inlet/exit widths specified by W/L=0.2, and with micro-channel widths equal to fin thicknesses. Larger numbers of manifold channels (smaller manifold spacing) dramatically reduces the temperature non-uniformity from the coolant temperature rise. Also, higher flow rates reduce the surface temperature variations, because: 1) the coolant temperature rise is less, and 2) for a given pump power the micro-channel widths are larger, and the coolant is not coupled as strongly to the fins. Shorter fins also reduce the coupling of the coolant to the fins. The <1°C lateral surface temperature uniformity requirement is easily met with either flow condition.

The vertical thermal resistance is shown in Fig. 9 as the laterally averaged top surface temperature minus the coolant inlet temperature for the same cases as in Fig. 8. The numbers on the curve points are the micro-channel widths. The micro-channel widths for the low flow rate case are twice as narrow as for the high flow rate case. This micro-channel width is the key to reducing the vertical thermal resistance. Larger numbers of manifold channels per unit width and taller fins (up to at least H_F/L=1) both improve the performance by allowing narrower micro-channel widths for a given pump power.

Fig. 10 shows the vertical thermal resistance for several inlet/exit widths. Wide inlets/exits (W/L=0.6) improve the performance allowing either a lower pump power or a lower vertical thermal resistance. The micro-channel widths largely determine the thermal resistance, and wider inlets/exits allow narrower micro-channels by not pinching the flow. Fig. 10 also indicates the thermal resistance limits due to the thin silicon and diamond layers (a diamond thermal conductivity value of 1250 W/m·K was used here) and due to the coolant temperature rise. The remaining thermal resistance is that for conducting the heat through the fins and transferring heat from the fins to the coolant. The fins perform very well.

Fig. 11 shows the effect of the ratio of fin thickness to micro-channel width on thermal resistance. The optimum points are for fin thicknesses that are about half the micro-channel width. Once again, the reason is that the flow resistance is reduced (by increasing the flow area) when the fins are thinner, so that the micro-channels and fins can both be thinner.

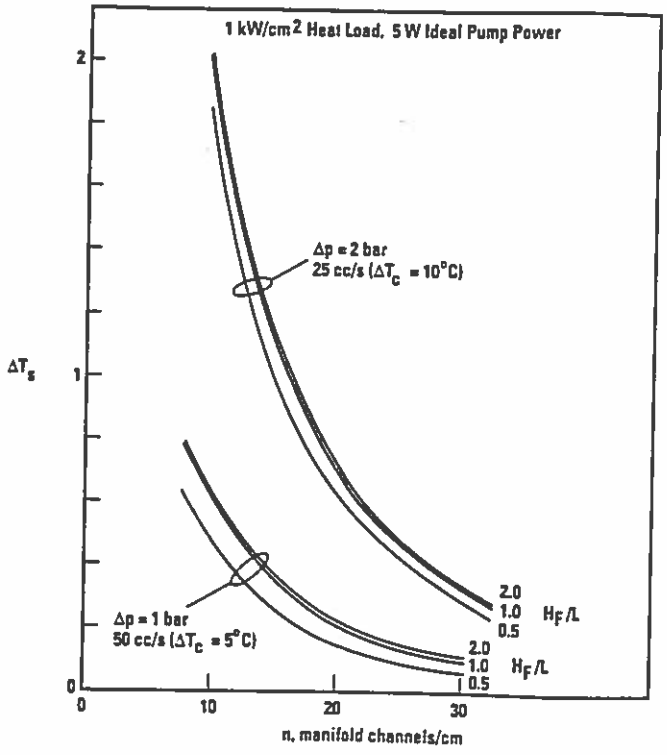

Fig.8 Lateral top surface temperature variation; more manifold channels give temperature uniformity.

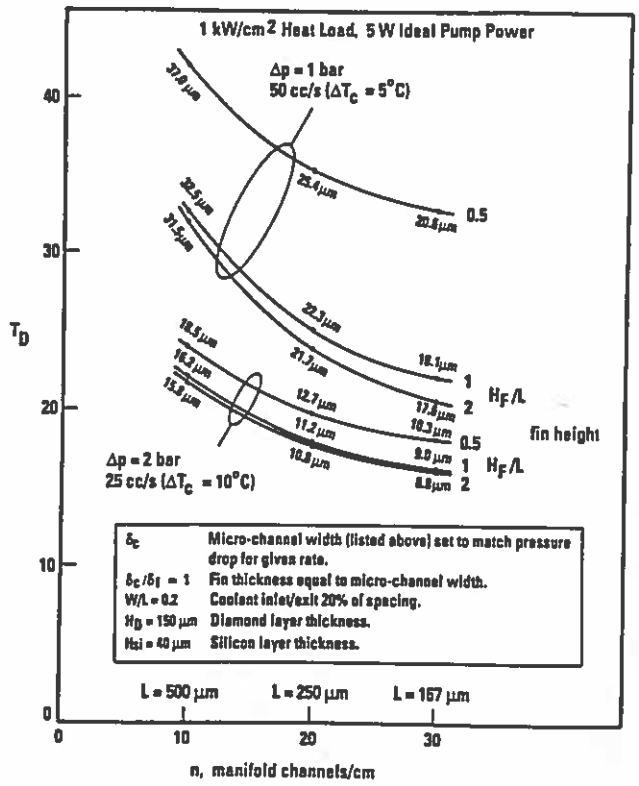

Fig.9 Surface temperature rise above coolant inlet: effect of number of manifold channels.

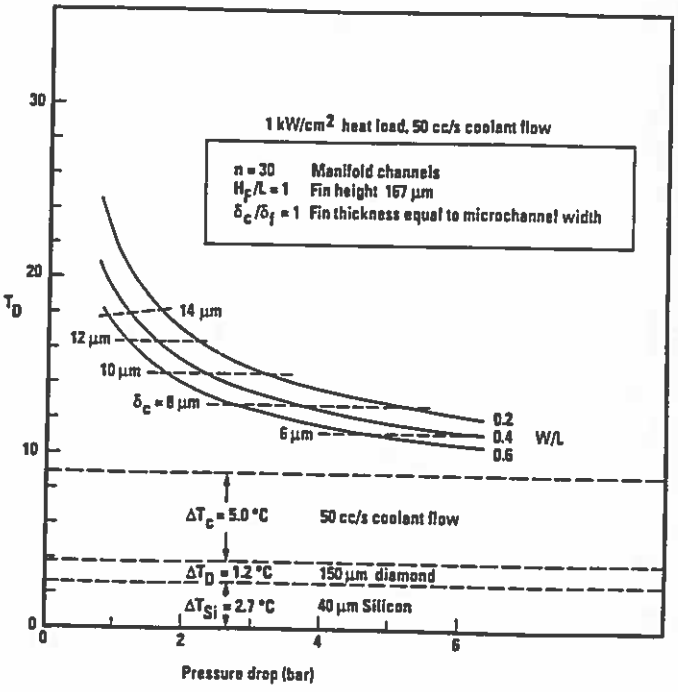

Fig.10 Surface temperature rise above coolant inlet: wider inlets/exits from manifold are better.

There are many ways to scale the present results for application to other parameter ranges. The temperatures all scale in proportion to heat flux if geometry and flow are fixed. However, for lower heat fluxes it may be advantageous to scale all geometrical dimensions up and the flow rate down in proportion to the heat flux (e.g., for 100 W/cm^2, 10x lower, use

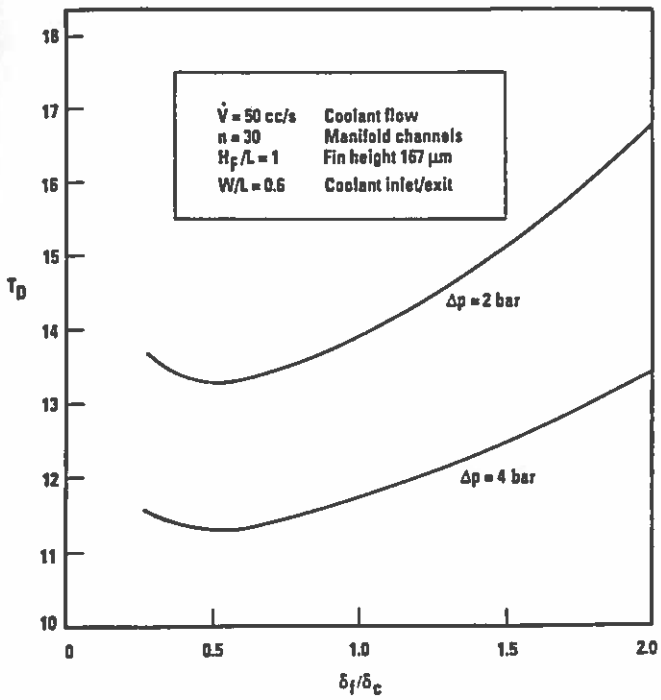

Fig.11 Surface temperature rise above coolant inlet: fins optimize thinner than micro-channels.

100 μm fin and channel thicknesses, 10x higher, and 5 cc/s flow rate per cm^2, 10x lower). This scaling leaves all the temperatures the same and reduces the pressure drop in proportion to the square of the heat flux reduction (0.01 bar, 100x lower). Thus, the pressure drop and the filtering requirements are reduced in designs for more modest heat fluxes.

Conclusions

A complete two-dimensional flow/thermal model of the micro-channel cooler has been developed. Optimization of the design parameters with this model has been demonstrated for the case of a 1 kW/cm^2 heat flux with the top surface at 25°C. For this case, pure water could be used as the coolant, or say 92% water/8% methanol (-5°C freezing point) if the heat is to be dumped to ice/water. The flow rate should be about 50 cc/s per cm^2 of surface area. The distribution manifold channel spacing (center-to-center) should be 333 μm (30 channels/cm). The fin height should be about 167 μm (H_F/L=1). The distribution manifold channel widths should be about 200 μm (W/L=0.6). The micro-channels should be between 7 μm and 14 μm wide, while the ratio of fin thickness to micro-channel width should be from 0.5 to 1.0. The top silicon layer should be thin (<50 μm). The diamond layer may not be needed until a non-uniform surface flux is specified (e.g., discrete diode laser strips). Lateral surface temperature non-uniformities due to just the coolant temperature rise are small when there are 30 manifold channels per cm. With these design parameters, an effective heat transfer coefficient (surface heat flux divided by surface to coolant inlet temperature difference) on the order of 100 W/cm^2K will be achieved with a total pressure drop of only about 2 bar.

Two words of caution are in order. First, beware of attaching a near perfect heat exchanger to a device that has its own significant thermal resistance between the heat source and the cooled surface. The perfect heat exchanger may not cure such a device. The device to be cooled and the heat exchanger will sometimes need to be designed together as a unit.

Second, the pressure drop for the flow in the manifold leading up to the micro-channels was not discussed yet, because the flow areas can usually be increased enough to make these pressure drops small in comparison to that through the micro-channels. However, the design must deliberately make these flow areas large. The supply and distribution manifolds can each have about 30% of their footprint open for the flow at each pressure level. Thus, the holes connecting the two can have 9% of the footprint open for each pressure level. Taking one dynamic head pressure loss in the inlet (high pressure side) and one head in the exit (low pressure side) between these two manifold layers adds to a 0.077 bar pressure loss for 25 cc/s or 0.31 bar pressure loss for 50 cc/s total flow rate per cm^2 of surface area. The distribution manifold channels should also be deep enough that the horizontal flow in this layer is not the limiting bottleneck area constriction.

Acknowledgment

This work was supported by Weapons Laboratory contract number F29601-90-C-0013. D. Mundinger and others at LLNL have helped by transferring the fabrication technology to TRW.

References

1. D.L. Kendall, "Vertical Etching of Silicon at Very High Aspect Ratios," Annual Review of Material Science, 9, 373-403 (1979).

2. D.B. Tuckerman and R.F.W. Pease, "High-Performance Heat Sinking for VLSI," IEEE Electron Device Letters, EDL-2(5), 126-129 (1981).

3. D.R. Mundinger, R. Beach, W. Benett, R. Solarz, V. Sperry, "Laser Diode Cooling for High Average Power Applications," LLNL UCRL-100245 (1989).